Acoustically driven ferroelastic domain switching observed by time-resolved x-ray diffraction

H. Navirian, H. Enquist, R. Nüske, A. Jurgilaitis, C. v. Korff Schmising, P. Sondhauss, and J. Larsson*
Department of Physics, Lund University, P.O. Box 118, SE-221 00 Lund, Sweden

(Received 3 November 2009; revised manuscript received 9 December 2009; published 26 January 2010)

Domain polarization switching in potassium dihydrogen phosphate (KH_2PO_4, KDP) induced by a propagating strain wave has been observed with time-resolved x-ray diffraction. A pulsed electric field with amplitude of 6 kV/cm and duration of 1 μs was applied along the crystallographic c axis. The field-induced strain waves emanating from the sample surfaces are the result of the converse piezoelectric effect. In the center of the probed surface two waves interfered constructively inducing ferroelastic domain switching, in the absence of an external electric field, at a delay of 3 μs, corresponding to acoustic propagation at a velocity found to be 1500 m/s.

DOI: 10.1103/PhysRevB.81.024113 PACS number(s): 77.65.−j, 61.05.cp, 77.80.Fm, 77.84.Fa

I. INTRODUCTION

Ferroelectric crystals have many applications in both science and technology. They are used, e.g., as components in computer memories,[1] as electro-optical devices,[2,3] and microsensors.[4] The relation between the microscopic structure of ferroelectrics and the observed mesoscopic and macroscopic properties has been studied. Optical techniques have been used to study the domain structure and the effects of external electric field, stress, and temperature.[5–8]

Potassium dihydrogen phosphate (KH_2PO_4, KDP) was one of the first ferroelectric materials to be discovered, and the theoretical modeling of ferroelectrics is based on studies of this material.[9,10] Experimental studies of KDP and isomorphs have included optical techniques,[11] x-ray scattering,[12] electron-spin resonance,[13] and neutron scattering.[14] Recently, the piezoelectric effect in paraelectric KDP at room temperature was studied at a third-generation synchrotron facility by Van Reeuwijk *et al.*[15] Grigoriev *et al.*[16,17] measured the domain dynamics of thin films of $[Pb(Zr,Ti)O_3]$, also known as PZT, which is ferroelectric at room temperature.

In the present work, time-resolved x-ray diffraction was used to study how high-amplitude strain waves induce ferroelastic domain switching in KDP just below the Curie temperature (T_C). Our work does not only demonstrate that it is possible to achieve sufficient amplitudes to induce domain switching but also demonstrates a way to measure the stress-strain relationship in ferroelastic materials. The acoustic strain waves were induced using the converse piezoelectric effect in a manner similar to that used by Van Reeuwijk *et al.* Close to T_C, the piezoelectric modulus is orders of magnitude higher than at room temperature, resulting in large-amplitude Rayleigh waves emanating from the corners when an electric pulse is applied. These strain waves have been observed to induce domain polarization switching. Rayleigh waves both rotate and strain the lattice planes. In the center of a surface though, the rotational components of Rayleigh waves coming from opposite ends compensate each other and only strain remains. This has been confirmed in simulations that are discussed later.

At room-temperature KDP has tetragonal symmetry and belongs to the space group $I\bar{4}2d$. When the crystal is cooled below T_C, it undergoes a phase transition to the ferroelectric phase, which has an orthorhombic symmetry and belongs to the $Fdd2$ space group. The unit-cell dimensions as shown in Fig. 1 are $a=10.5459(9)$ Å, $b=10.4664(10)$ Å, and $c=6.9265(21)$ Å at 20 K below T_C.[18] Unless otherwise stated we will use a coordinate system with axes (x,y,z) parallel to the axes of the ferroelectric unit cell a, b, and c. This will be referred to as the ferroelectric coordinate system as shown in Fig. 1. The standard coordinate system for the parelectric phase is rotated by 45° around the common z axis compared to the ferroelectric coordinate system. The structural change in KDP at T_C is explained by the double-well potential of the hydrogen bond between the oxygen atoms that link the PO_4 groups. This is discussed in the review article by Nelmes.[19] Above T_C, the hydrogen atoms move freely between the two potential minima. Below it, the thermal energy of the hydrogen atoms is not sufficient to overcome the potential barrier and hence they remain on one side or the other. As a consequence, the hydrogen bonds become asymmetric, which affects the internal structure of the phosphate groups as well as the position of the potassium ion. The structural changes in turn affect the unit cell, which undergoes shear deformation (in the paraelectric coordinate system). The displacement of the phosphor and potassium atoms results in a permanent dipole moment along the c axis. The dipole moments in the

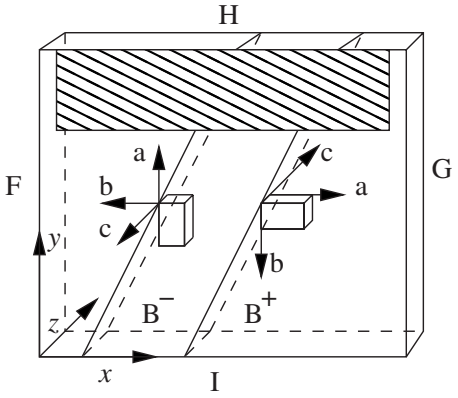

FIG. 1. Sample geometry. The sample was coated with gold electrodes as indicated by the shaded box close to surface H. The orthorhombic unit cell dimensions (a, b, and c) are drawn for the two studied domain types. Sample surfaces are marked as F, G, H, and I.

A^+ and B^+ domains are in the same direction, which is opposite to the direction of the dipole moments in the A^- and B^- domains.

II. EXPERIMENTAL SETUP

The experiment was carried out at beamline D611 at the MAX-laboratory synchrotron facility in Lund (Sweden), which provides x rays in the range 3–10 keV. A double-crystal Si (111) monochromator was used to obtain 4.3 keV x rays with a bandwidth of $\Delta E/E=2.0\times10^{-4}$. The x-ray footprint on the sample was 1×0.2 mm^2. The KDP sample had dimensions of $10\times10\times1$ mm^3 along the a, b, and c axes, respectively, and was mounted on a cryogenically cooled manipulation stage so that the position in all three spatial directions, and the incidence angle could be changed. The crystal was cooled to about 3 K below T_C which is known to be 123 K. The temperature was measured by a diode-based temperature sensor mounted in contact with the sample. The measured fluctuations were less than 0.2 K. Any systematic dependence from applying the electric pulses was less than that. However, it is difficult to measure the absolute temperature, so all temperatures are given relative to T_C. The KDP 220 Bragg reflection was studied, where the Miller indices are given in the paraelectric $I\bar{4}2d$ basis corresponding to the 400 reflection in the ferroelectric $Fdd2$ basis. This is henceforth referred to as the 400 reflection. The sample was symmetrically cut, i.e., the probed reciprocal-lattice vector was parallel to the surface normal. The Bragg angle was 30°. In this setup the x-ray penetration depth was 6 μm, limited mainly by absorption.

An electrical field was applied parallel to the c axis by means of gold electrodes which were evaporated directly onto the crystal. Square voltage pulses were applied with a duration of 1 μs at a 500 Hz repetition rate. The rise time of the high voltage was on the order of 100 ns. An avalanche photodiode (APD S5343LC5, Hamamatsu) with a time resolution of about 1 ns and active area of 1 mm^2 was used to detect the x rays reflected off the KDP crystal. The x-ray energy was scanned and the diffracted intensity was recorded as a function of time for each energy step using a LeCroy WaveMaster 8500 oscilloscope. Each such transient building up the time-resolved energy scan is the average of 570 events. Scanning the energy is a convenient way of recording a rocking curve as long as there are no absorption edges nearby and the scanning range is small. Scanning the diffraction angle would require scanning of the small fast detector.

III. EXPERIMENTAL METHOD

As can be seen in Fig. 2 the single paraelectric peak splits into four separate peaks in the ferroelectric phase. This is due to the fourfold rotation-inversion ($\bar{4}$) symmetry axis of the paraelectric phase. Thus, there are four different ways in which the structure can be transformed, and hence four possible domain types with a permanent dipole moment can exist below T_C. These domains are termed A^+, A^-, B^+, and B^- according to the definition used by Bornarel.[20] Below T_C, the 400 reciprocal-lattice vectors of the four domain types

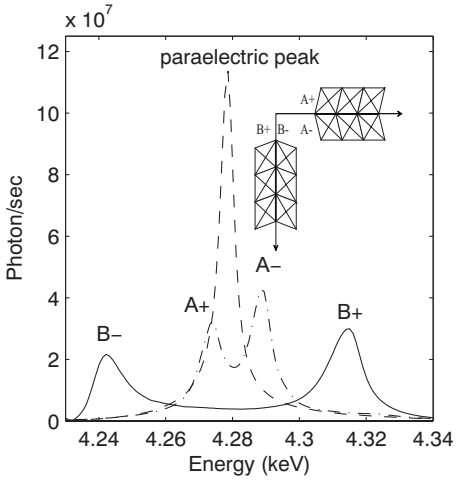

FIG. 2. X-ray energy scan. A paraelectric peak at room temperature (dashed line), B^+ and B^- peaks (solid lines), A^+ and A^- peaks (dashed-dotted line). We also show the domain orientation for the four main domain types (Ref. 20). The representation is in the paraelectric coordinate system.

have different orientations and magnitudes (see Fig. 3). Each of the domains fulfills the Bragg condition at a different x-ray energy for a certain angle of incidence. Figure 2 shows three energy scans at the same angle of incidence. One scan was taken above T_C and shows the paraelectric peak. The other two scans were recorded below T_C and show the ferroelectric peaks. In these two scans the sample has been conditioned by cycling the temperature and by applying a dc field in order to produce either A^+ and A^- domains or B^+ and B^- domains, Fig. 3.

We use the relative intensity of the peaks to measure the volume ratio of the different domain types. The interpretation of the intensity as a measure of the volume ratio is unam-

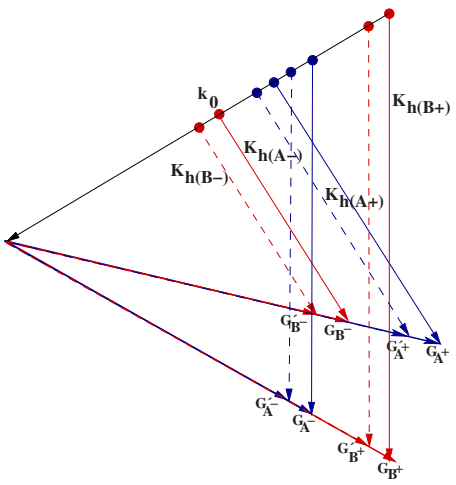

FIG. 3. (Color online) Vector representation of Bragg's law for the different domain types in KDP. The incoming wave vector (K_0) is shown together with the scattered wave vectors ($K_{h(B^+)}, K_{h(B^-)}, K_{h(A^+)}, K_{h(A^-)}$). The 400 reciprocal-lattice vectors for the different domain types are also drawn as solid lines. A strain modifies the lattice vectors (shown as dashed lines) and thereby the scattering vectors.

biguous under our conditions. First, we have observed experimentally that domains are much smaller than the x-ray footprint on the sample which confirms previous measurements of domain size to be about 10 μm by Bonarel[6] and others.[21,22] This excludes the possibility that the intensity variation is due a few large domains moving in and out from the 1 mm probe area. Second there are no effects from x-ray scattering efficiency changes. Since we are making energy scans and the integrated intensity is evaluated, shifts cannot significantly change the intensity of the scattered radiation. Shifts of 5 eV can change the structure factor by only by 0.5% whereas the changes observed are as large as 50%.

IV. MODEL

Applying a homogeneous electric field to a KDP crystal results in homogeneous stress due to the converse piezoelectric effect, giving rise to a homogeneous strain defined by[23]

$$\eta_i = d_{ji} E_j, \tag{1}$$

where d_{ji} is the piezoelectric modulus and E_j is the applied electric field.

When the electric field is switched on and off, the relaxation of the piezoelectric stress generates Rayleigh waves that emanate from the corners of the crystal and propagate along the surfaces. In the paraelectric coordinate system the pure shear strain for the initially applied electric field (6 kV/cm) is calculated to be 9×10^{-4} using Eq. (1) and the piezoelectric tensor given by Lüdy.[24] In the ferroelectric coordinate system, it corresponds to a tensile strain of 4.5×10^{-4}. The temporal profiles of the acoustic wave essentially mimic the temporal evolution of the electrical pulse. In order to fully understand the acoustic conditions in the experiments, two-dimensional simulations were carried out using the finite element method (FEM). The simulations take into account the piezoelectric and elastic tensors of KDP, the size and orientation of the crystal and the size of the gold coating. Waves propagating along the c axis had been neglected in order to reduce the computational costs. The simulation shows that on the probed surface a Rayleigh surface wave propagates. As expected, we observe that the displacement of the wave is rotating and that the direction of rotation differs between the waves emanating from either edge. At the center of the probed surface, where interference of the two waves occurs the horizontal parts cancel out and a vertical displacement giving rise to a vertical strain remains. The time evolution of the strain at the center of the probed surface is plotted in Fig. 4. The full movie showing the strain propagation is available online.[25] The velocity of Rayleigh waves in KDP has been found to be 1500 m/s (Ref. 26) which means that the strain pulses are only 1.5 mm long. The simulations also show that the electric pulses induce bell-mode oscillations in KDP, i.e., resonance of the crystal as a whole. The displacement of an atom by these bell modes can be significant but the strain (the gradient of the displacement) is small for these long-wavelength modes. The strain-generation mechanism is quite similar to the work by Thomsen *et al.*[27] who studied laser-induced low-dispersion waves using optical techniques. Later such low-dispersion strain waves have been extensively studied by x-ray scattering techniques,[28–32] and the probing techniques for measuring these propagating waves are nearly identical to the work described here.

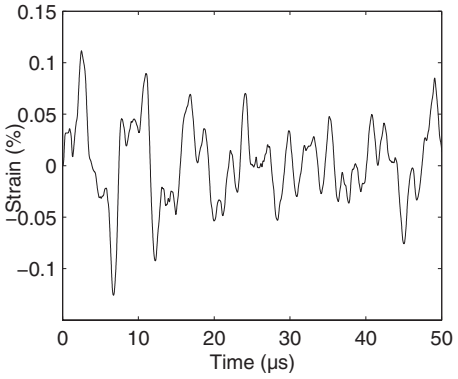

FIG. 4. Simulated evolution of the strain in the probe region from an FEM model. It is in good agreement with the measured shift of the B^+ and B^- peaks.

The strain can experimentally be observed in the energy scans as shifts of the peaks representing the different domain types. As seen in the FEM simulations, the excited acoustic waves do not induce any significant rotation of lattice planes in the middle of the surface H where they are probed. So the change in peak position can be readily used to evaluate the strain.

The tensile stress, σ, can be calculated from the strain using Hook's law and the elastic tensor, C, for the ferroelectric phase

$$\boldsymbol{\sigma} = \mathbf{C}\,\boldsymbol{\eta}. \tag{2}$$

For the geometry employed in this experiment, strain in y direction (η_y) is parallel to the normal of surface H. The stress in y direction is negligible due to the free surface. The strain η_y can be calculated from the tensile stress along the x axis using the elastic tensor using Eq. (2).

Care must be taken not to induce temperature effects via the applied electric field. However, no dc peak shift was observed when applying the pulsed voltage to the sample, which agrees with the temperature sensor measurement. Furthermore the signature is different as a temperature change moves the ferroelectric peaks closer or further away from the center of gravity whereas the acoustic wave moves them in the same direction (toward higher or lower energy, depending on whether it is expansive or compressive strain).

V. MEASUREMENTS AND RESULTS

A time-resolved energy scan showing the effect of the acoustic waves is shown in Fig. 5. The diffracted intensity is coded in false color. The data were obtained by probing the center of the sample. Due to the conditioning of the sample the probe volume consists of only two domain types, B^+ and B^-. The B^+ domains have diffraction peaks at higher energy. The B^+ signal is stronger, indicating that there is a larger volume fraction of B^+ domains in the probe volume. When a voltage of 6 kV/cm is applied with a polarity which we will refer to as positive, an initial shift of each peak is observed.

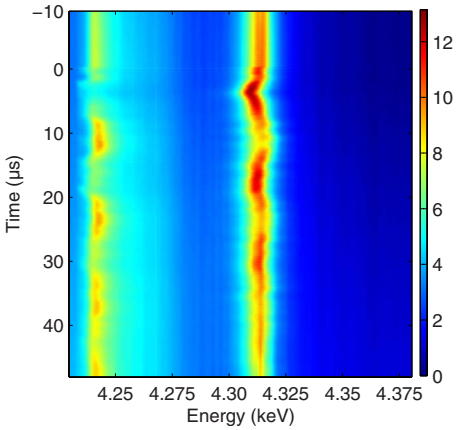

FIG. 5. (Color online) Diffracted intensity as a function of time and x-ray energy. The signal at 4.24 keV corresponds to the B^- domain and the signal at 4.31 keV comes from the B^+ domains. The data were recorded following a positive 600 V pulse with 1 μs duration starting at time $t=0$. The center of the crystal was probed.

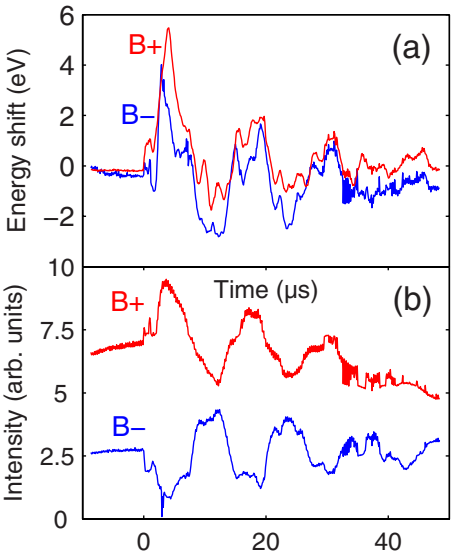

FIG. 6. (Color online) (a) Position and (b) integrated intensity of the diffraction peaks of the B^+ and B^- domains derived from the data in Fig. 5.

This shift follows the 1 μs pulse shape of the electrical pulse. This is consistent with a longitudinal wave propagating from the H surface (Fig. 1). Approximately 3 μs later, a shift is observed which is twice as large. This arises from the interfering Rayleigh waves emanating from the corners. When these waves are reflected at the respective opposite surfaces their phase changes from expansion to compression, and as they travel back to the probe area a shift in the opposite direction is seen. This is repeated several times with a period of 13 μs determined by the propagation time in the crystal. Knowing the dimensions of the crystal, the speed of the waves in the crystal was calculated to be 1500 m/s, which is in agreement with the room temperature measurement by Bakos *et al.*[26] Another striking feature of the data is that expansive strain is accompanied by enhancement of the B^+ integrated peak intensity and a corresponding decrease in the B^- peak, indicating a smaller fraction of B^- domains. Similarly, compressive strain induces enhancement of the B^- signal at the expense of B^+ intensity.

In order to understand these observations and to analyze them quantitatively we note that in a ferroelastic material, strain is made up from two contributions. The first is a contribution proportional to the stress and the second one comes from domain reversal. In KDP a full domain reversal corresponds to a 0.76% change in strain. We will from here on refer to these contributions as the linear strain and the ferroelastic strain, respectively. Hence, the amplitude of the linear strain can be evaluated from the shift in the energy of each peak and the amplitude of the ferroelastic strain can be evaluated by the relative integrated peak intensities from the two domain types as shown in Fig. 6. As discussed in the experimental methods section, the integrated intensity of each domain peak is a measure of the fraction of that particular domain type in the probe volume.

Since the electric field is applied along the crystallographic c axis the only nonzero element of the piezoelectric modulus is d_{36}. The matrix element, d_{36}, in the tetragonal paraelectric coordinates couples the electric field along the crystallographic c axis to linear pure shear strain in the plane normal to the c axis. The piezoelectric modulus, d_{36} has been investigated by Lüdy.[24] It shows an anomaly and increases from 23.2 pC/N at 20 °C to 1470 pC/N at T_C which is the value used in our calculations since the temperature variation in d_{36} below T_C is small. The linear shear strain at the applied field of 6 kV/cm can be calculated, and it corresponds to a linear tensile strain of 4.5×10^{-4} corresponding to a tensile stress of 620 N/cm^2 in the rotated ferroelectric coordinate system. This is in excellent agreement with the present experimental study, where the initial strain from the shift in the energy was found to be 5×10^{-4}. The strain after 3 μs is twice as large (10^{-3}) since we probed the center of the upper surface, where Rayleigh waves emanating from the top corners of the crystal interfere constructively. Near the surface, this corresponds to a tensile stress perpendicular to the strain which is 3100 N/cm^2. When probing an area off-center by more than 0.75 mm, where no interference can occur, the peak energy shifts and changes in x-ray intensity are less prominent and more complex due to the rotary displacement vectors which are present. Attempts to induce higher stress by increasing the voltage resulted in sample damage, which was manifested as a crack in the exact center of the crystal where the interference occurred.

The stress-strain relation for ferroelastic materials is described by a hysteresis loop.[33] As shown above, the stress can be calculated from the linear strain. The ferroelastic strain can be derived from the relative integrated peak intensities of the two domain types. Hence we can plot the stress-strain relation from the data in Figs. 5 and 6.

The measured stress-strain relationship of KDP is shown in Fig. 7. The stress was not sufficient to observe actual hysteresis. However, the deviation from linear behavior is obvious. The points in Fig. 7 are experimental data and are built up by all the time points in Fig. 6. The stress (x axis in the Fig. 7) was calculated from the linear strain which was directly measured by the shift in peak energy of the B^+ domains using Eq. (2). The integrated peak intensities were

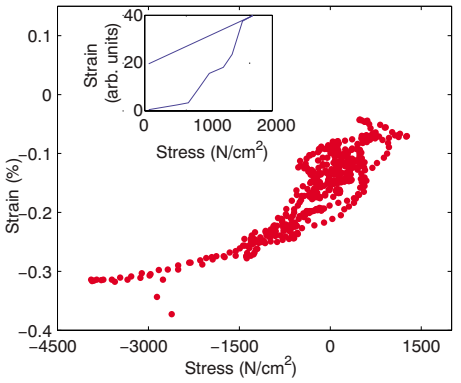

FIG. 7. (Color online) Measured stress-strain relation for KDP at $T_C=3$ K. The data from Ref. 34 is added as an inset.

determined for each time point. They provide the ferroelastic strain which is the main contribution to the strain in Fig. 7. The deviation from a linear stress-strain relation is an indication of ferroelastic hysteresis, although we do not observe a significant difference in strain depending on if stress is increasing or decreasing. The only ferroelastic measurement previously carried out for this brittle material has been added for comparison. That measurement was carried out using electron paramagnetic resonance in Cr^{+3}-doped KDP.[34] We show the data from Ref. 35 as an inset to Fig. 7 since the strain scale was arbitrary in that paper.

VI. DISCUSSION

The switching process can be understood from the ideas of Slater[9] and Yosama and Nagamiya.[10] The Gibbs free energy can be written as

$$U = \frac{1}{2}Na\eta^2 - \varepsilon^s N - \beta\eta(N^+ - N^-) - (N^+ - N^-)\mu E - TS, \tag{3}$$

where N^+ and N^- denote the number of $(H_2PO_4)^-$ dipoles in the unit cells belonging to domains with polarity parallel or antiparallel to the c axis, a is a number proportional to the normal elastic constant, and N is the total number of dipoles. The first term stands for the elastic energy, which is the same for both domain types. The second term represents the interaction of dipoles with each other, where ε^s is a constant parameter. The third term was introduced by Yosama and Nagamiya.[10] It describes a correction to the elastic energy which has opposite signs for the two domain types and β is a constant. This term is the most important when discussing ferroelastic switching. The fourth term was introduced by Slater[9] to account for the reorientation of domains of dipole moment μ in an external electric field (E). T is the temperature and S is the entropy which is a function of N, N^+, and N^-.

The domain ratio follows from the minimization of the free energy. In the absence of external fields or forces the crystal will have an equal fraction of domains with opposing polarization in order to compensate the depolarizing fields. In the presence of an external field or forces the equilibrium ratio changes and domain switching occurs in order to minimize the free energy. Domain switching in ferroelectric materials has been studied extensively and has been found to occur in different ways: through nucleation of a reverse polarization domain, through domain propagation in the direction of the electric field, and through domain growth in the direction perpendicular to the electric field.[15,35]

In our experiment the field is turned off after 1 μs by grounding both electrodes, and the electrodes will rapidly redistribute the surface charges to compensate for the polarization induced by the piezoelectric effect as the strain waves propagate. This means that there is no macroscopic external field present. In Eq. (3), the term including the electric field is zero while the ferroelastic term is independent of the field. Hence, we find that the mechanism responsible for domain switching is ferroelastic rather than ferroelectric. We have experimentally observed that expansive strain is accompanied by the increase in B^+ domains and compressive by that of B^-. This is consistent with the fact that the factor β in Eq. (3) is positive as predicted by the original calculations.[10] In conclusion, we have generated and observed high-amplitude strain waves in the ferroelectric phase of KDP, and that these waves drive domain polarization switching in the absence of an electric field.

ACKNOWLEDGMENTS

The authors would like to thank the Swedish Research Council (VR), the Knut and Alice Wallenberg Foundation, the Crafoord Foundation, the Carl Trygger Foundation, and the European Commission via the Marie Curie Program, for their financial support.

*jörgen.larsson@fysik.lth.se

[1] H. Ishiwara, M. Okuyama, and Y. Arimoto, *Ferroelectric Random Access Memories: Fundamentals and Applications* (Springer, New York, 2004).
[2] S. Liu and X. Min, Appl. Phys. Lett. **88**, 143512 (2006).
[3] D. A. Scrymgeour and V. Gopalan, Phys. Rev. B **72**, 024103 (2005).
[4] P. Muralt, J. Micromech. Microeng. **10**, 136 (2000).
[5] J. Bornarel and R. Cach, Phys. Rev. B **60**, 3806 (1999).
[6] J. Bornarel, J. Appl. Phys. **43**, 845 (1972).
[7] J. Bornarel and J. Lajzerowicz, Ferroelectrics **4**, 177 (1972).
[8] P. Bastie, J. Bornarel, J. Lajzerowicz, M. Vallade, and J. R. Schneider, Phys. Rev. B **12**, 5112 (1975).
[9] J. Slater, J. Chem. Phys. **9**, 16 (1941).
[10] S. Yomosa and T. Nagamiya, Prog. Theor. Phys. **4**, 263 (1949).
[11] M. Vallade, Phys. Rev. B **12**, 3755 (1975).
[12] K. Ståhl, Å. Kvick, and S. C. Abrahams, Acta Crystallogr., Sect. A: Found. Crystallogr. **46**, 478 (1990).

[13] R. C. DuVarney and R. P. Kohin, Phys. Rev. Lett. **20**, 259 (1968).
[14] N. Pérès, M. Souhassou, B. Wyncke, G. Gavoille, A. Cousson, and W. Paulus, J. Phys.: Condens. Matter **9**, 6555 (1997).
[15] S. J. van Reeuwijk, A. Puig-Molina, O. Mathon, R. Tucoulou, and H. Graafsma, J. Appl. Phys. **94**, 6708 (2003).
[16] A. Grigoriev, D.-H. Do, D. M. Kim, C.-B. Eom, B. Adams, E. M. Dufresne, and P. G. Evans, Phys. Rev. Lett. **96**, 187601 (2006).
[17] A. Grigoriev, R. Sichel, H. N. Lee, E. C. Landahl, B. Adams, E. M. Dufresne, and P. G. Evans, Phys. Rev. Lett. **100**, 027604 (2008).
[18] R. J. Nelmes, Z. Tun, and W. F. Kuhs, Ferroelectrics **71**, 125 (1987).
[19] R. J. Nelmes, Ferroelectrics **71**, 87 (1987).
[20] J. Bornarel, Ferroelectrics **71**, 255 (1987).
[21] R. M. Hill and S. K. Ichiki, Phys. Rev. **135**, A1640 (1964).
[22] J. Bornarel and J. Lajzerowicz, J. Appl. Phys. **39**, 4339 (1968).
[23] J. F. Nye, *Physical Properties of Crystals* (Clarendon Press, Oxford, 1957).
[24] W. Lüdy, Z. Phys. **113**, 302 (1939).
[25] See supplementary material at http://link.aps.org/supplemental/10.1103/PhysRevB.81.024113 for a movie showing the strain evolution in the crystal.
[26] J. S. Bakos Zs. Sörlei, Cs. Kuti, and S. Szikora, Appl. Phys. A: Mater. Sci. Process. **19**, 59 (1979).
[27] C. Thomsen, H. T. Grahn, H. J. Maris, and J. Tauc, Phys. Rev. B **34**, 4129 (1986).
[28] C. Rose-Petruck, R. Jimenez, T. Guo, A. Cavalleri, C. W. Siders, F. Raksi, J. A. Squier, B. C. Walker, K. R. Wilson, and C. P. J. Barty, Nature (London) **398**, 310 (1999).
[29] A. M. Lindenberg, I. Kang, S. L. Johnson, T. Missalla, P. A. Heimann, Z. Chang, J. Larsson, P. H. Bucksbaum, H. C. Kapteyn, H. A. Padmore, R. W. Lee, J. S. Wark, and R. W. Falcone, Phys. Rev. Lett. **84**, 111 (2000).
[30] P. Sondhauss, O. Synnergren, T. N. Hansen, S. E. Canton, H. Enquist, A. Srivastava, and J. Larsson, Phys. Rev. B **78**, 115202 (2008).
[31] J. Larsson, A. Allen, P. H. Bucksbaum, R. W. Falcone, A. Lindenberg, G. Naylor, T. Missalla, D. A. Reis, K. Scheidt, A. Sjögren, P. Sondhauss, M. Wulff, and J. S. Wark, Appl. Phys. A: Mater. Sci. Process. **75**, 467 (2002).
[32] P. Sondhauss, J. Larsson, M. Harbst, G. A. Naylor, A. Plech, K. Scheidt, O. Synnergren, M. Wulff, and J. S. Wark, Phys. Rev. Lett. **94**, 125509 (2005).
[33] E. K. H. Salje, *Phase Transition in Ferroelastic and Co-elastic Crystals* (Cambridge University Press, Cambridge, 1990).
[34] T. Kobayashi, J. Phys. Soc. Jpn. **35**, 558 (1973).
[35] E. Fatuzzo, Phys. Rev. **127**, 1999 (1962).